Information Flow of Cascading Bacterial Molecular Communication Systems with Cooperative Amplification

Samitha S. Somathilaka
Walton Institute
Waterford Institute of Technology
Waterford, X91 P20H, Ireland
samitha.somathilaka@waltoninstitute.ie

Daniel P. Martins
Walton Institute
Waterford Institute of Technology
Waterford, X91 P20H, Ireland
daniel.martins@waltoninstitute.ie

Sasitharan Balasubramaniam
School of Computing
University of Nebraska-Lincoln
Lincoln, NE, USA
sasi@unl.edu

***Abstract*—Bacterial ecosystems are integrated with cascading molecular communications networks that contain redundant paths transmitting molecular signals through a shared medium, resulting in accumulation of diverse molecules. Due to a range of factors, including residual noise and channel attenuation, the information flow between bacterial populations can be affected. Although the cooperative transceiver bacterial populations in parallel paths of the network amplify molecular signals to overcome channel attenuation, it further minimises the residual noise by absorbing higher signal molecules resulting in reliable information flow through the network. In this study, using information and molecular communications theory, we investigate the impact of Cooperative Amplification (CA) on InterSymbol Interference (ISI) in Bacterial Molecular Communication Networks (BMCN) with redundant paths. Moreover, we analyse the information flow through a cascading and parallel molecular communications system that uses different molecules as signals. We first show the effect of CA on the ISI and then the reliability of bacterial molecular networks using a vital metabolic functionality of the Human Gut Bacteriome (HGB), which is Short Chain Fatty Acids (SCFA) production. The analysis on the CA shows that the performance of the network can be enhanced up to a certain level by increasing the number of cooperate transceivers. Finally, the estimated Mutual Information (MI) for each bacterial population for three different networks using the data generated from simulations, indicates that the molecular communication network with redundant paths can support reliable information flow despite significant molecular residual noise.**

***Index Terms*—Molecular communication, Bacterial networks, Mutual information, Residual noise, Parallel communications channels, Metabolic pathways, Cooperative amplification.**

I. Introduction

The Human Gut Bacteriome (HGB) is the bacterial ecosystem residing in the human gut and considered as a virtual organ [1] due to its involvement in critical metabolic tasks of the host through molecular interactions [2]. This results in formation of a complex molecular interaction network containing a large number of nodes and interactions through various molecular species, as illustrated in Figure 1. Hence, we identify this network as a Molecular Communications (MC) network that contains the interactions of a massive amount of channels with numerous molecular species. MC is an emerging field with a plethora of novel applications, especially in the biological field, such as biosensing and biocomputing [3], [4]. Some of the characteristics of HGB environment contrast the behaviors of MC from the conventional communication system, such as the production of residual noise. This process occurs due to the incomplete utilization of molecular species found in HGB environments [5]. Therefore, the residual noise has been modelled in MC systems as ISI, where a molecular signal emitted in a specific time slot will interfere with the decodification of the next [6]. Moreover, this effect has an enlarged impact in cascading MC networks due to the number of parallel transmitters sending molecular signals towards a single receptor.

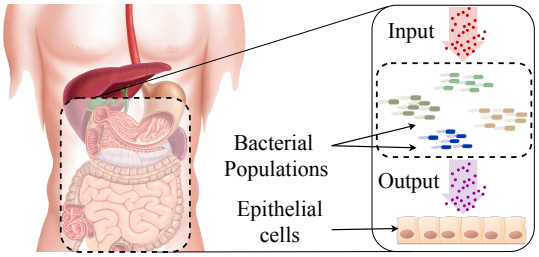

Fig. 1: The figure illustrates how the HGB receive molecular inputs and convert them into output signals. Finally, the output signal is being received by the host's epithelial cells.

In addition to the residual noise, the exchange of molecules in the HGB can also suffer from Brownian noise due to molecular displacement [7]. Therefore, it is crucial to investigate the dynamics of the communications that support the bacterial networks in HGB when subjected to such types of noise. To this day, many studies have investigated the effects of noise in diffusive communications channels. For instance, an analysis of diffusion-based noise source that affects end-to-end MC systems was developed in [8]. Further, Moore et al. [9] modelled residual noise and introduced two approaches for noise reduction in order to achieve higher information rates. The effect of molecular noise on the channel capacity has been analysed by Nakano et al. [10], where they consid-

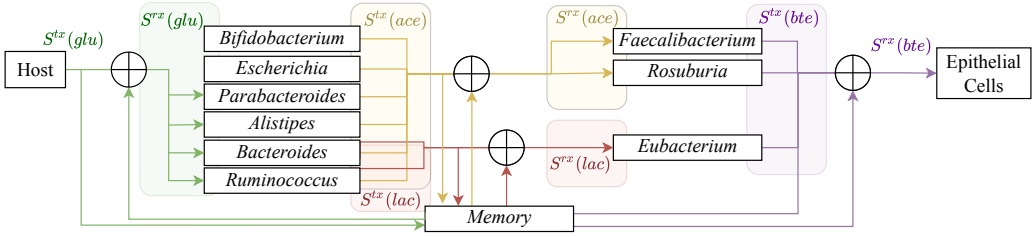

Fig. 2: Bacterial cascading system of SCFA production with the environment memory component. $S^{tx}(glu)$, $S^{tx}(ace)$, $S^{tx}(lac)$ are the transmitted and $S^{rx}(glu)$, $S^{rx}(ace)$, $S^{rx}(lac)$ and $S^{rx}(bte)$ are the received glucose, acetate, lactate and butyrate signals respectively that are affected by the noise from the memory.

ered a nanomachine transmitter placed in a one-dimensional molecular communication channel (they assumed that the molecular propagation via Brownian motion would degrade over time) [10]. In a different direction, molecular noise analysis targeting specific application such as drug delivery systems have also been proposed. For example, Chahibi and Akyildiz [11] conducted a noise analysis of the nano-particle propagation based on a long-term drug distribution throughout the body. Here, we extend these works to investigate the effects of both residual and Brownian noises on a Bacterial Molecular Communication Network.

This paper investigates the reliability of BMCN considering parallel molecular signal transceivers as cooperative amplifiers, which are identified as multiple nodes coordinating and transmitting the same signal and amplifying it to improve the range of transmission [12]. Although CA is a solution to overcome the channel attenuation [13], it may increase the residual noise and ISI, reducing the performance of the BMCN. To investigate this phenomenon, we use a sub-network of HGB, where cascading communications are required for the production of Short Fatty Chain Acids - SCFA (SCFA is one of the most important metabolic functions of the HGB [14]) as shown in Figure 2. The bacterial populations represented in Figure 2 were selected after a careful investigation on real data obtained from MicrobiomeDB [15]. Furthermore, we investigate the performance of our proposed cascading MC system through the evaluation of the MI (using a method inspired by [16]) for each one of the communications links involved in this sub-network. Our model also takes into account the accumulation effect that occurs in an MC channel when multiple sources produce a large number of molecules, approximating our investigation to the real production of SCFA by the bacterial populations in HGB.

The rest of the paper is organized as follows. Section II explains the system dynamics of the considered cascading sub-network of the HGB, and Section III focuses on the analysis conducted on the mentioned system. Next, in Section IV we discuss the final results and conclude the paper in Section V.

II. Cascading Molecular Communication System

The MC interaction network of the HGB is a collection of numerous metabolic paths. Each path consists of multiple bacterial populations (i.e., molecular transceivers or nodes) that can receive molecular signals from a node, process them and release another type of molecular signal to the next node. The molecular signal processing can be described as follows, $M_1 + M_2 \underset{k_r}{\overset{k_f}{\rightleftharpoons}} M_3$ where M_1, M_2 and M_3 are the molecules, k_f and k_r are the forward and reverse reaction rates. If the reaction is non-reversible, $k_r = 0$.

The molecular propagation between two nodes in the HGB environment is affected by various factors such as molecular noise [8]. In cascading molecular communication systems, the magnitude of noise impact is expanded with the progression through cascading layers as each layer has its own noise component. If the cascading channels use the same type of molecules, the issue becomes more significant as the diffusion medium facilitates increased accumulation. Nevertheless, this study focuses only on a BMCN that uses different types of molecules for cascading layers, as shown in Figure 2.

In diffusion based MC channels, only a certain portion of emitted molecules reach the particular receiver within a respective time frame. The rest of them accumulate in the environment and act as residual noise (Figure 3) causing ISI.

III. Information Flow Analysis

The analysis on the bacterial MC network of this study is structured to investigate the impact of CA on residual memory and the reliability of the network in terms of information flow. First, we analyse how the CA changes the residual memory resulting in alterations of ISI. Later, MI is calculated to understand the information flow through the network.

A. Intersymbol interference analysis

As shown in Figure 2, the considered system contains parallel paths that transmit the same signal through the system. This phenomenon can be identified as CA [13], and it can affect the ISI levels experienced by the investigated system. To investigate this relationship, we first use a generic setup that contains multiple bacterial nodes cooperating to amplify the molecular signals. Then, we apply the obtained results to the evaluation of the SCFA production. Here, we measure the ISI by calculating the interference signal to total signal strength ratio [6], as follows.

$$ISI = \frac{\sum_{k=0}^{K} \sum_{a_0=1}^{A_0} q^{rx}_{(B_k,a_0)}}{\sum_{k=0}^{K} \sum_{a_0=0}^{A_0} q^{rx}_{(B_k,a_0)} + \sum_{k=0}^{K} \sum_{a_1=0}^{A_1} q^{rx}_{(B_k,a_1)}} \quad (1)$$

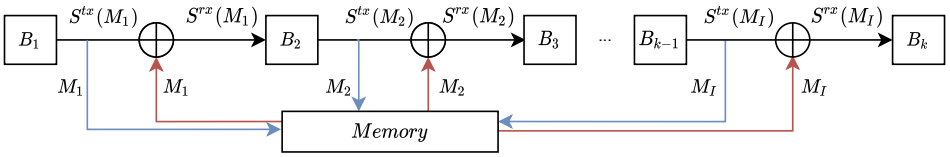

Fig. 3: Cascading communication system with channel memories causing residual noise

where $q^{rx}_{(B_k,a_0)}$ and $q^{rx}_{(B_k,a_1)}$ are the number of molecules received by the bacterial population B_k $(k = 0, 1, ..., K)$ for a_0th bit $(a_0 = 0, 1, ..., A_0)$ and a_1th bit $(a_1 = 0, 1, ..., A_1)$ for "0" and "1" symbols, respectively.

B. Mutual information analysis

In addition to investigating the relationship between CA and ISI, this study explores the information flow capabilities of BMCN in the HGB. Here, we estimate the MI of the cascading BMCN for the butyrate production for three different scenarios (control, Autism, and Parkinson's disease average compositions). Butyrate is one of the most important SCFA, and it can be considered as the primary energy source for the colon epithelial cells. Further, it has the properties for immunomodulation and anti-inflammation [17].

We model the butyrate as the final product of a cascading BMCN containing nine bacterial genera, and this selection of bacterial populations takes into account their similarities between metabolic functionalities and ancestral origins. The butyrate production starts from the glucose input into the HGB, as illustrated in Figure 2, and we can identify four layers in this system: 1) host - glucose transmitters, 2) acetate/lactate producers - consume glucose and produce acetate/lactate, 3) butyrate producers - consume acetate/lactate and produce butyrate, and 4) epithelial cells - butyrate receivers. For such configuration, the *Bacteroides, Alistipes, Parabacteroides, Bifidobacterium, Ruminococcus* and *Escherichia* genera receive glucose and transmit acetate. Moreover, the *Faecalibacterium* and *Roseburia* genera receive acetate, and *Eubacterium* receives lactate to produce butyrate. Finally, the epithelial cells receive butyrate signals produced by the bacterial populations. This bacterial ecosystem is implemented (as shown in Figure 2) on our simulations by combining the literature curated data on metabolism and compositional data from MicrobiomeDB.

We can break down the nine bacterial genera (i.e., nodes) into a combination of series and parallel communications links and investigate the interactions between pairs of nodes. This combination is our cascading BMCN model, which can be seen in Figure 3 (representation of one of the communications links required for the butyrate production). Considering one channel between two bacterial genera, i.e. pair p, in the cascading system that uses a M_i molecule as the signalling molecule, we calculate the MI of this interaction I_p as follows,

$$I_p = H(S^{tx}_h) - H(S^{tx}_h|\{S^{rx}_{B_k}(t),\ t_0 \le t \le t_{max}\}). \tag{2}$$

where $H(S^{tx}_h)$ is the estimated entropy of the input signal, S^{tx} from the host and $H(S^{tx}_h|S^{rx}_{B_k})$ is the estimated conditional entropy of input signal S^{tx}_h given the received signal $S^{rx}_{B_k}$ by the bacterial population B_k, where tx and rx are the identifiers for the transmitted and received signals, respectively.

We generate data for different input concentrations $c_j, j = 1, ..., J$ of the input signal S^{tx}. For each concentration, the simulator iterated R times with T number of time steps. We utilise the data obtained from these iterations to compute the entropy of the glucose input signal $H(S^{tx}_h)$ using a histogram approach [18], [19] as follows,

$$H(S^{tx}_h) = -\sum_{j=1}^{J} p_{S^{tx}_h}(c_j) \log_2 \left(\frac{p_{S^{tx}_h}(c_j)}{w_{S^{tx}_h}} \right) \tag{3}$$

where $p_{S^{tx}_h}(c_j) = 1/J$ is the probability of each input concentration c_j, J is number of input concentrations, and

$$w_{S^{tx}_h} = \frac{\max(c_j) - \min(c_j)}{J}, \tag{4}$$

is the sample interval for the input signal. Using (3)-(4), we compute the conditional entropy as follows

$$\begin{aligned} &H(S^{tx}_h|\{S^{rx}_{B_k}(t),\ t_0 \le t \le t_{max}\}) = \\ &-\sum_{N_{B_k,t_0}} \sum_{N_{B_k,t_1}} \cdots \sum_{N_{B_k,t_{max}}} p_{S^{rx}_{B_k}}(\alpha) \\ &\cdot \sum_{s=1}^{S_\alpha} p_{S^{tx}_h|\alpha}(c_j) \log_2 \left(\frac{p_{S^{tx}_h|\alpha}(c_j)}{w_{S^{tx}_h \alpha}} \right) \end{aligned} \tag{5}$$

where $\alpha = \{c^{rx}_{B_k,t}\}_{t=0}^{t_{max}}$ is the set of concentrations of the received signal S^{rx} through out the considered simulation time steps, N_{B_k,t_n} is the number of bins of the received signal $S^{rx}_{B_k}$ used to generate the multi-dimensional histogram $p_{S^{rx}_{B_k}}(\alpha)$, V_α is the number of histogram bins used to generate the multi-dimensional histogram $p_{S^{tx}_h|\alpha}(c_j)$ while $w_{S^{tx}_h,\alpha}$ which is calculated as,

$$w_{S^{tx}_h,\alpha} = \frac{\max(c_j) - \min(c_j)}{V_\alpha}. \tag{6}$$

Moreover, N_{B_k,t_n} is calculated as follows to the nearest integer [19],

$$N_{B_k,t_n} = 1 + \log_2(U) + \log_2 \left(1 + \frac{g_\beta}{\sigma_{g_\beta}} \right) \tag{7}$$

where $\beta = c^{rx}_{B_k}(t_n)$ is the concentration of the received signal by B_k at time t_n of , $U = J \cdot R$ is the number of simulation runs, and g_β is estimated skewness of the distribution of $P_{S^{rx}_{B_k}}$ while σ_{g_β} is calculated as,

$$\sigma_{g_\beta} = \sqrt{\frac{6(U-2)}{(U+1)(U+3)}}. \tag{8}$$

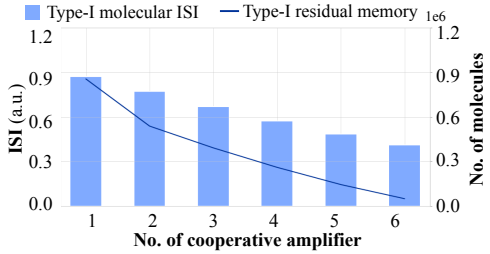

Fig. 4: Impact of the CA on the residual memory and ISI

Using the same approach to calculate the number of bins of the received signal in (7), we calculate the number of histogram bins for the input signal V_α to the nearest integer, which is represented as,

$$V_\alpha = 1 + \log_2(I) + \log_2\left(1 + \frac{g_{c_j}}{\sigma_{g_{c_j}}}\right), \tag{9}$$

where g_{c_j} is estimated skewness of the distribution of c_j and,

$$\sigma_{g_{c_j}} = \sqrt{\frac{6(I-2)}{(I+1)(I+3)}}. \tag{10}$$

IV. Results

In this section, we show the analytical results for ISI against CA and results for the MI of the investigated BMCN. We generated data for these analyses using a bacterial ecosystem simulator that we developed based on real data collected from several microbiome databases available online, such as MicrobiomeDB and NJS16 [5]. The simulator is used to conduct *in silico* experiments and generate data on bacterial interactions. It has a 3D environment (dimensions: $150 \times 150 \times 150\,\mu$m) with a static medium where molecules propagate via diffusion. Mainly, this diffusion induces the stochastic nature of the system. The simulator utilises a voxel architecture to discretise the environment for precise data generation on the transmission and reception for each molecular species. Further, the simulator was fined tuned by using an array of iterative experiments to match the average production behaviours of SCFA in human GB (for further details on the extraction of the average behaviour, please refer [20]). We utilise this configuration to approximate our simulation to *in vivo* or *in vitro* experiments on SCFA production/consumption in the HGB.

A. Intersymbol interference vs cooperative amplification

In order to investigate the impact of multiple transceivers on the signal amplification and how it affects the residual memory indirectly, we use a generic setup with six experiments. The first setup only contains one transceiver and developed the other five setups by increasing the number of cooperate transceivers up until six. We used the same input signal with four "1" bits (where bit "1" represented by the transmission of molecules and bit "0" by not transmitting any molecule) of molecule type-I from TX with a fixed amplitude for each setup. The transceivers receive type-I molecules and transmit type-II signal to the receiver RX. Figure 4 shows the results of the signal behaviours due to CA. When the number of cooperative transceivers increases in the environment, they absorb more molecules resulting minimised probability of molecular accumulation. Reduction of accumulation reflects in ISI. When there is only one transceiver in the environment, Figure 4 shows the accumulation of Type-I molecules is high, and similarly, ISI is also high. With the increment of the cooperative transceivers, it is clearly evident that the amount of Type-I residual memory decreases and the ISI of Type-I also reduces. Therefore, it can be concluded that in MC, CA can be considered as a solution for ISI.

Further, we extended the analysis to evaluate the signal reception behaviour by an individual transceiver, signal strength of cooperative transmission and the received signal strength at the end of the system. As shown in Figure 5, here we only focus on a single pulse to clearly observe the variations. In Figure 5a it is evident that when the number of transceivers increases in the environment the possibility of signal reception of each node degrades. Nevertheless, the transmitted signal from the transceivers collectively amplifies until a certain concentration of transceivers in the environment (in this setup, the maximum strength of the transmitted signal is in the setup with four transceivers) as shown in the Figure 5b. Hence, Figure 5c explains there is a maximum strength that can be expected by increasing the number of cooperative transceivers.

B. Analytical results for information flow

BMCNs in the HGB suffers from the same noise impact we discussed in previous sections, but they are equipped with redundant paths through parallel transceiver bacterial populations that can be considered as cooperative amplifiers. The composition of the HGB differs for each individual, and the scale of CA relies on the compositions as well. Therefore, we estimated the information flow for the control, autistic and Parkinson's HGBs average compositions.

We initiate the simulator with the Relative Abundance (RA) of each genus, which is calculated based on the species level RA found in the data analysed from MicrobiomeDB and Disbiome [21] databases. We followed the same procedure on the sample data from the Disbiome database to define the average compositions related to two diseases, autism and Parkinson's disease. Next, we introduce twenty single pulse glucose inputs with different concentration ranging from $0.259\,\mu\text{mol}/\text{m}^3\text{s}$ to $2.594\,\mu\text{mol}/\text{m}^3\text{s}$ to start the production of molecules in the second layer of our cascading MC model for all three setups (control, autism and Parkinson's). The amplitudes of the molecular inputs were selected based on the number of bacterial cells we implemented on our simulator to get results with clear changes in the information flow. Above and below that range, results does not indicate any significant changes. The simulation duration was set to 500 minutes by observing the strongest (glucose input) and the weakest (lactate input) signal behaviours in order to have all the significant changes of signals within the mentioned time frame. Further, each setup

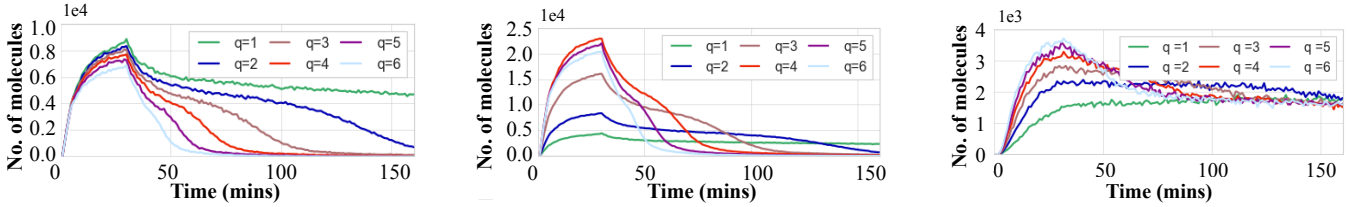

(a) (b) (c)

Fig. 5: Illustration of CA by simultaneous transceivers where (a) Number of type-I molecules received per transceiver, (b) total number of type-II molecules produced of q number of transceivers and (c) number of type-II molecules received by the end receiver.

iterated for 50 arbitrary times to increase the accuracy of the results over the system stochasticity and collected the data of molecular consumption and production of each bacterial population for all time steps.

Figure 6 depicts the behaviours of all the four input signals. Figure 6a shows the ten out of twenty single pulse glucose inputs to the system, while Figure 6b exhibits the combination of the acetate transmission by *Bacteroides*, *Alistipes*, *Parabacteroides*, *Bifidobacterium*, *Ruminococcus* and *Escherichia*, which is several times weaker than the glucose signal. The strength of the signal transmitted by these bacteria genera relies on the number of acetate-producing bacterial cells and the quality of signal reception by the next layer of this cascading MC system. Compared to the acetate signal, lactate and butyrate signals are significantly weaker, but with a preserved waveform as shown by Figures 6c and 6d. These signals are used to compute the performance of the information flow on this cascading BMCN.

First, we compute the input signal entropy and conditional entropy of the cascading BMCN using (3) and (5) respectively for each setup. Then, the conditional entropy for all nine bacteria genera were estimated in three steps for each setup. First, the conditional entropy for the *Bacteroides*, *Alistipes*, *Parabacteroides*, *Bifidobacterium*, *Ruminococcus* and *Escherichia* genera were computed considering glucose input signals. Then, the conditional entropy for *Faecalibacterium* and *Roseburia* genera were evaluated based on the data generated for their acetate reception. Finally, conditional entropy for lactate channel of *Eubacterium* genera and butyrate reception by epithelial cells were also computed. This step is required for the evaluation of the MI for these bacterial interactions. MI for each bacterial interaction is calculated using (2) and the results for each bacterial population is shown in Figure 7.

The results in Figure 7a, 7b and 7c, elucidate that, with the compositional changes, information flow differ through the network. The set of glucose receivers is considered the first layer of cooperative amplifiers and the acetate and lactate receivers as the second layer of cooperative amplifiers in this cascading system. The estimated MIs of first layers of three compositions differ significantly. The estimated MIs in the second layer show a lesser variation compared to the first layer, and at the end, MI of epithelial cells have close values for all

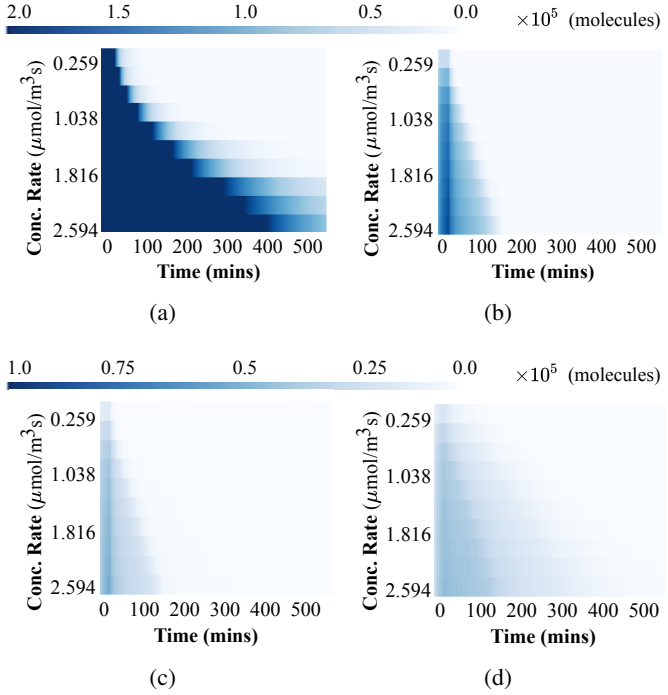

(a) (b) (c) (d)

Fig. 6: Input signal behaviours for the considered time frame of (a) glucose, (b) acetate, (c) lactate and (d) butyrate signals for all the glucose input concentrations. Note that (c) and (b) are with a lower scale compared to (a) and (b).

three setups. The maximum value of MI is from *Bacteroides* in all setups, as it dominates the ecosystems RA-wise. Interestingly, transceivers' MIs of a layer tend to have higher values compared to those of the previous layer. This highlights, in systems with redundant paths through cooperative transceivers, higher information flow can be expected.

These results show that the use of CA is an important mechanism to support a reliable information flow through BMCN. This opens up possibilities to utilise concepts and techniques currently applied to multi-path wireless communications to improve the performance of cascading MC systems.

V. Conclusion

Similarly to conventional communications systems, the performance of MC systems can suffer from ISI. In a BMCN,

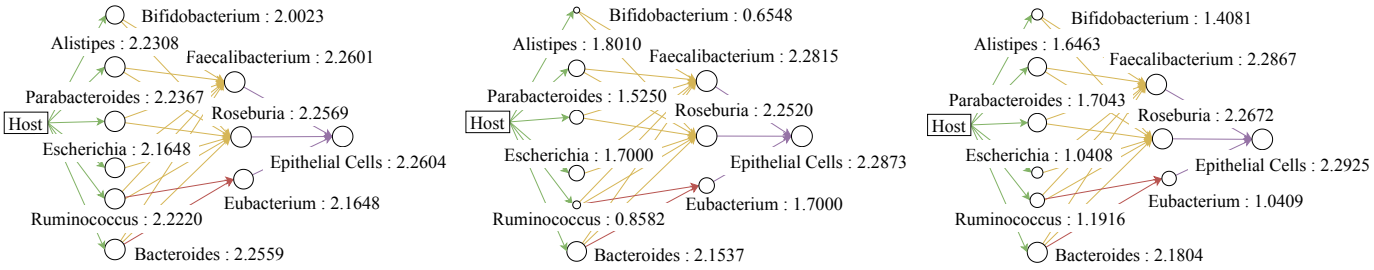

Fig. 7: Estimated MI values for each bacterial population and epithelial cells for (a) control HGB, (b) parkinson's HGB and (c) autistic HGB. Sizes of nodes represent the corresponding MI values in bits.

such as the one created in the HGB to metabolise SCFA, this is translated into multiple cascading molecular noises. Hence, in this study, we have considered this effect to investigate the information flow through a cascading MC system required for butyrate production. Here, we show that the problem of residual noise can be addressed up to a certain content using CA. At the same time, we also could observe, through the MI results, that the natural architecture created in HGB to produce butyrate makes this cascading BMCN more robust against such molecular noises. Furthermore, the MI results highlight that multipath communication with CA is an important mechanism to maintain the performance of a cascading BMCN in the HGB, which opens the possibility of implementing wireless techniques associated with indoor propagation to improve such MC systems. The obtained results contribute to the future design of a more reliable cascading BMCN that can send and receive information from the body. Reliable information transmission from/to the body is essential in smart drug delivery and smart diagnostics systems.

ACKNOWLEDGEMENT

This publication has emanated from research conducted with the financial support of Science Foundation Ireland (SFI) and the Department of Agriculture, Food and Marine on behalf of the Government of Ireland under Grant Number [16/RC/3835].

REFERENCES

[1] J. M. Evans, L. S. Morris, and J. R. Marchesi, "The gut microbiome: the role of a virtual organ in the endocrinology of the host," *J Endocrinol*, vol. 218, no. 3, pp. R37–47, 2013.

[2] S. Sanna, N. R. van Zuydam, A. Mahajan, A. Kurilshikov, A. V. Vila, U. Võsa, Z. Mujagic, A. A. Masclee, D. M. Jonkers, M. Oosting, *et al.*, "Causal relationships among the gut microbiome, short-chain fatty acids and metabolic diseases," *Nature genetics*, vol. 51, no. 4, pp. 600–605, 2019.

[3] T. Nakano, M. J. Moore, F. Wei, A. V. Vasilakos, and J. Shuai, "Molecular communication and networking: Opportunities and challenges," *IEEE Transactions on NanoBioscience*, vol. 11, no. 2, pp. 135–148, 2012.

[4] D. Bi, A. Almpanis, A. Noel, Y. Deng, and R. Schober, "A survey of molecular communication in cell biology: Establishing a new hierarchy for interdisciplinary applications," *IEEE Communications Surveys Tutorials*, vol. 23, no. 3, pp. 1494–1545, 2021.

[5] J. Sung, S. Kim, J. J. T. Cabatbat, S. Jang, Y.-S. Jin, G. Y. Jung, N. Chia, and P.-J. Kim, "Global metabolic interaction network of the human gut microbiota for context-specific community-scale analysis," *Nature communications*, vol. 8, no. 1, pp. 1–12, 2017.

[6] M. U. Mahfuz, D. Makrakis, and H. T. Mouftah, "Characterization of intersymbol interference in concentration-encoded unicast molecular communication," in *2011 24th Canadian conference on electrical and computer engineering (CCECE)*, pp. 000164–000168, IEEE, 2011.

[7] S. K. Tiwari and P. K. Upadhyay, "Maximum likelihood estimation of snr for diffusion-based molecular communication," *IEEE Wireless Communications Letters*, vol. 5, no. 3, pp. 320–323, 2016.

[8] M. Pierobon and I. F. Akyildiz, "Capacity of a diffusion-based molecular communication system with channel memory and molecular noise," *IEEE Transactions on Information Theory*, vol. 59, no. 2, pp. 942–954, 2012.

[9] M. J. Moore, T. Suda, and K. Oiwa, "Molecular communication: Modeling noise effects on information rate," *IEEE Transactions on NanoBioscience*, vol. 8, no. 2, pp. 169–180, 2009.

[10] T. Nakano, Y. Okaie, and J.-Q. Liu, "Channel model and capacity analysis of molecular communication with brownian motion," *IEEE Communications Letters*, vol. 16, no. 6, pp. 797–800, 2012.

[11] Y. Chahibi and I. F. Akyildiz, "Molecular communication noise and capacity analysis for particulate drug delivery systems," *IEEE Transactions on Communications*, vol. 62, no. 11, pp. 3891–3903, 2014.

[12] S. Abadal, I. Llatser, E. Alarcón, and A. Cabellos-Aparicio, "Cooperative signal amplification for molecular communication in nanonetworks," *Wireless networks*, vol. 20, no. 6, pp. 1611–1626, 2014.

[13] I. Llatser, A. Cabellos-Aparicio, and E. Alarcon, "Networking challenges and principles in diffusion-based molecular communication," *IEEE Wireless Communications*, vol. 19, no. 5, pp. 36–41, 2012.

[14] Y. P. Silva, A. Bernardi, and R. L. Frozza, "The role of short-chain fatty acids from gut microbiota in gut-brain communication," *Frontiers in endocrinology*, vol. 11, p. 25, 2020.

[15] C. Huttenhower, D. Gevers, R. Knight, S. Abubucker, J. H. Badger, A. T. Chinwalla, H. H. Creasy, A. M. Earl, M. G. FitzGerald, R. S. Fulton, *et al.*, "Hmp phase i (v3-v5)," 2012.

[16] A. Gohari, M. Mirmohseni, and M. Nasiri-Kenari, "Information theory of molecular communication: directions and challenges," *IEEE Transactions on Molecular, Biological and Multi-Scale Communications*, vol. 2, no. 2, pp. 120–142, 2016.

[17] A. Rivière, M. Selak, D. Lantin, F. Leroy, and L. De Vuyst, "Bifidobacteria and butyrate-producing colon bacteria: importance and strategies for their stimulation in the human gut," *Frontiers in microbiology*, vol. 7, p. 979, 2016.

[18] A. Papoulis, *Probability, random variables, and stochastic processes*. Boston: McGraw-Hill, 2002.

[19] Z. Sakkaff, A. Immaneni, and M. Pierobon, "Estimating the molecular information through cell signal transduction pathways," in *2018 IEEE 19th International Workshop on Signal Processing Advances in Wireless Communications (SPAWC)*, pp. 1–5, IEEE, 2018.

[20] S. S. Somathilaka, D. P. Martins, W. Barton, O. O'Sullivan, P. Cotter, and S. Balasubramaniam, "A graph-based molecular communications model analysis of the human gut bacteriome," *IEEE Journal of Biomedical and Health Informatics*, pp. 1–1, 2022.

[21] Y. Janssens, J. Nielandt, A. Bronselaer, N. Debunne, F. Verbeke, E. Wynendaele, F. V. Immerseel, Y.-P. Vandewynckel, G. D. Tré, and B. D. Spiegeleer, "Disbiome database: linking the microbiome to disease," vol. 18, June 2018.